Water for food: The global virtual water trade network

M. Konar,[1] C. Dalin,[1] S. Suweis,[1,2] N. Hanasaki,[3] A. Rinaldo,[2,4] and I. Rodriguez-Iturbe[1]

Received 6 December 2010; revised 15 February 2011; accepted 24 February 2011; published 17 May 2011.

[1] We present a novel conceptual framework and methodology for studying virtual water trade. We utilize complex network theory to analyze the structure of the global virtual water trade associated with the international food trade. In the global virtual water trade network, the nations that participate in the international food trade correspond to the nodes, and the links represent the flows of virtual water associated with the trade of food from the country of export to the country of import. We find that the number of trade connections follows an exponential distribution, except for the case of import trade relationships, while the volume of water that each nation trades compares well with a stretched exponential distribution, indicating high heterogeneity of flows between nations. There is a power law relationship between the volume of virtual water traded and the number of trade connections of each nation. Highly connected nations are preferentially linked to poorly connected nations and exhibit low levels of clustering. However, when the volume of virtual water traded is taken into account, this structure breaks down. This indicates a global hierarchy, in which nations that trade large volumes of water are more likely to link to and cluster with other nations that trade large volumes of water, particularly when the direction of trade is considered. Nations that play a critical role in maintaining the global network architecture are highlighted. Our analysis provides the necessary framework for the development of a model of global virtual water trade aimed at applications ranging from network optimization to climate change impact evaluations.

Citation: Konar, M., C. Dalin, S. Suweis, N. Hanasaki, A. Rinaldo, and I. Rodriguez-Iturbe (2011), Water for food: The global virtual water trade network, *Water Resour. Res.*, *47*, W05520, doi:10.1029/2010WR010307.

1. Introduction

[2] Global freshwater resources are finite and subject to increasing pressures from population growth, economic development, and climate change [*Vorosmarty et al.*, 2000; *Gleick*, 2008; *Strzepek and Boehlert*, 2010]. The vast majority (90%) of global freshwater use is for food production [*Shiklomanov*, 1997; *Oki and Kanae*, 2004; *Hoekstra and Chapagain*, 2008], which is why much attention and research has been devoted to the use of water in agriculture. In fact, there is a growing body of literature that focuses on the water that is embodied in the production and trade of agricultural commodities, referred to as "virtual water." Since the concept was first introduced by *Allan* [1993], there has been a dramatic increase in the virtual water literature, largely in an attempt to quantify its potential to alleviate regional water scarcity and save water globally [*Chapagain et al.*, 2006; *Yang et al.*, 2006; *D'Odorico et al.*, 2010].

[3] International trade links the fortunes and resources of countries, providing potentially important conduits for geographically limited water resources to be transferred to water-stressed regions. The virtual water trade between regions [*Hoekstra and Hung*, 2005; *Chapagain et al.*, 2006; *Yang et al.*, 2006; *Hanasaki et al.*, 2010] and the gross virtual water flow of nations [*Chapagain and Hoekstra*, 2008] have been quantified. These studies have focused primarily on agricultural commodities [*Hoekstra and Hung*, 2005; *Liu et al.*, 2007; *Rost et al.*, 2008; *Hanasaki et al.*, 2010], including those used for biofuel production [*Gerbens-Leenes et al.*, 2009], but the concept has also been extended to include industrial products [*Chapagain and Hoekstra*, 2008]. However, the global properties of virtual water trade have not yet been quantified or explored. In this paper we build upon the virtual water literature and utilize complex network methods to characterize the global structure of the virtual water trade associated with the international food trade.

[4] The origin of complex network theory can be traced back to the work of *Erdös and Rényi* [1961] on random graphs. Recently, much research has been devoted to the field of complex network analysis, both theoretically and as applied to real-world systems [*Barabási and Albert*, 1997; *Newman et al.*, 2006]. This recent interest in complex networks is largely due to the discovery of organizing principles in networks [*Costa et al.*, 2007], such as community structure [*Watts and Strogatz*, 1998] and scale-free properties [*Barabási and Albert*, 1997]. Additionally, network analysis has become increasingly popular because of its

[1]Department of Civil and Environmental Engineering, Princeton University, Princeton, New Jersey, USA.
[2]Laboratory of Ecohydrology, ECHO/IEE/ENAC, École Polytechnique Fédérale de Lausanne, Lausanne, Switzerland.
[3]National Institute for Environmental Studies, Tsukuba, Japan.
[4]Department IMAGE and International Centre for Hydrology "Dino Tonini," Università di Padova, Padua, Italy.

0043-1397/11/2010WR010307

flexibility and generality for representing many natural structures [*Barabási*, 2002; *Costa et al.*, 2007], including street systems [*Kalapala et al.*, 2006; *Masucci et al.*, 2009], the internet and World Wide Web [*Barabási and Albert*, 1997], international tourism [*Miguens and Mendes*, 2008], financial transactions [*Garlaschelli and Loffredo*, 2005; *Kyriakopoulos et al.*, 2009], Hollywood actors, and scientific collaborations [*Newman*, 2001; *Barrat et al.*, 2004], among others.

[5] We present a novel application of network theory to the global virtual water trade. The global virtual water trade forms a weighted and directed network in its complete representation. A weighted network is one in which values are associated with the links of the network, while a directed network is one where the links connect nodes in a particular direction [*Wasserman and Faust*, 1994; *Newman*, 2003; *Newman et al.*, 2006; *Jackson*, 2008]. For the virtual water trade network, the links are assigned a weight on the basis of the volume of virtual water that is traded between countries and a direction according to the direction of the underlying commodity trade flow (i.e., from exporter nation to importing nation). In this paper, we study the virtual water trade network associated with the trade of 58 agricultural commodities from five major crops (i.e., barley, corn, rice, soy, and wheat) and three major livestock products (i.e., beef, pork, and poultry) in the year 2000. These products account for approximately 60% of global calorie consumption (Food and Agriculture Organization of the United Nations (FAO), FAOSTAT, 2010, http://faostat.fao.org/site/291/default.aspx, hereinafter referred to as FAOSTAT, 2010). There are 166 nations that participate in the export of these commodities and 151 that import these commodities, comprising the nodes of the network. The volume of virtual water that is traded globally is 625×10^9 m^3 yr^{-1}, which accounts for approximately 10% of the global freshwater use in agriculture, or 8% of total global water use [*Hoekstra and Chapagain*, 2008].

[6] Complex network theory has been used to characterize the world trade web weighted by the financial value of traded commodities (e.g., refer to *Garlaschelli and Loffredo* [2005], *Fagiolo et al.* [2008], *Kyriakopoulos et al.* [2009], and *Barigozzi et al.* [2010]). In this paper, we analyze the network structure of global virtual water trade associated with the international food trade. Thus, we apply the tools of complex network theory to a subset of the world trade web. However, the major departure between our analysis and other network studies of world trade centers on the weights (i.e., value) assigned to the trade flows. We assign weights to links in the international food trade on the basis of the volumes of water embodied in a given trade relationship, while other studies of the world trade web in the literature assign weights in terms of financial values [*Garlaschelli and Loffredo*, 2005; *Fagiolo et al.*, 2008; *Kyriakopoulos et al.*, 2009; *Barigozzi et al.*, 2010]. Additionally, we analyze both the directed and weighted properties of the network, which is seldom done in the literature, with rare exceptions like the work of *Miguens and Mendes* [2008].

[7] Scientific understanding of natural hydrological processes has dramatically increased over the past 50 years [*Oki and Kanae*, 2004]. Now a similar quantitative representation of the social aspects of water use is necessary. With this goal in mind, we analyze the global structure of virtual water trade. The network analysis presented here highlights global properties of virtual water trade jointly with individual roles and mutual interactions of single nations within the overall network architecture. Not only is this type of analysis fascinating in its own right, but it is our hope that future extensions of this work will illuminate unprecedented opportunities to save water globally and serve as a tool for impact assessment, particularly under future scenarios of climate change, whose impacts on the linked water and food systems will likely be captured by changes in global virtual water flows. In particular, in order to develop a theoretical network model [*Suweis et al.*, 2011] that may account for the structural features of real-world virtual water trade, we must first be able to frame what those features are [e.g., *Newman et al.*, 2006]. Hence, a thorough analysis of empirical data of the type presented in this paper is essential.

2. Building the Global Virtual Water Trade Network

[8] Here we describe the construction of the global virtual water trade network. In the network, each country participating in food trade is represented by a node. Links between nodes are directed on the basis of the direction of trade flow and are weighted by the volume of virtual water embodied in the traded commodities. To construct this network, we require two main pieces of information: the crop trade between all nations and the virtual water content of each crop in all nations. For a complete list of the commodities considered in this paper refer to Table 1. We obtain the bilateral trade of agricultural products from the FAO. To calculate the virtual water content of the commodities, we utilize the H08 global hydrological model [*Hanasaki et al.*, 2008a, 2008b]. Virtual water flows between nations are then calculated by multiplying the international trade flow of a particular commodity by the associated virtual water content of that commodity in the country of export.

2.1. Virtual Water Content Data

[9] We calculated the virtual water content of five unprocessed crops (barley, corn, rice, soy, and wheat) and three livestock products (beef, chicken, and pork) for each nation by water withdrawal source using the H08 global hydrological model [*Hanasaki et al.*, 2008a, 2008b]. Virtual water content (VWC, kg water kg^{-1} product) of raw crops is defined as the evapotranspiration during a cropping period (kg m^{-2}) divided by the crop yield (kg m^{-2}). The VWC of unprocessed livestock products is defined as the water consumption per head of livestock (kg head^{-1}) divided by the livestock production per head (kg head^{-1}). A brief description of the H08 model is provided here; for further information the interested reader is referred to *Hanasaki et al.* [2010].

[10] The H08 model consists of six modules: land surface hydrology, river routing, crop growth, reservoir operation, environmental flow requirements estimate, and anthropogenic water withdrawal. The model operates on a $0.5° \times 0.5°$ grid spatial resolution with water and energy balance closure. Two types of input data are necessary to run the H08 model: meteorological forcing and land use. Using the H08 model, we are able to assess the two major sources of virtual water content: precipitation ("green water") and irrigation ("blue water") [*Falkenmark and Rockstrom*, 2004].

Table 1. List of Commodities and the Yield Ratio r, Price Ratio p, and Content Ratio c[a]

	Ratio		
	r	p	c
Crop Commodities			
Wheat	1	1	1
Flour of wheat	0.78	0.97	1
Bran of wheat	0.22	0.024	1
Macaroni	0.78	0.97	1
Germ of wheat	0.025	0.01	1
Bread	0.78	0.97	0.71
Bulgur	1	1	1
Rice, paddy	1	1	1
Rice, husked	0.72	1	1
Milled husked rice	0.72	1	1
Rice, milled	0.65	0.95	1
Rice, broken	0.65	0.95	1
Bran of rice	0.07	0.049	1
Rice, bran oil	0.013	0.049	1
Cake rice bran	0.057	0.049	1
Rice, flour	0.65	0.95	1
Rice, fermented beverages	0.48	0.95	0.36
Barley	1	1	1
Pot barley	0.46	0.76	1
Barley, pearled	0.46	0.76	1
Bran of barley	0.54	0.24	1
Barley flour and grits	0.46	1	1
Malt	0.78	1	1
Malt extract	0.78	1	0.8
Beer of barley	0.78	1	0.14
Maize	1	1	1
Germ of maize	0.115	0.18	1
Flour of maize	0.8	0.75	1
Bran of maize	0.085	0.068	1
Maize oil	0.04	0.18	1
Cake of maize	0.075	0.18	1
Soybeans	1	1	1
Soybean oil	0.19	0.35	1
Cake of soybeans	0.76	0.65	1
Soya sauce	0.76	0.65	0.17
Maize, green	1	1	1
Maize for forage and silage	1	1	1
Livestock Products			
Cattle meat	0.6	0.61	1
Offal of cattle, edible	0.32	0.38	1
Fat of cattle	0.04	0.0024	1
Meat cattle boneless (beef and veal)	0.6	0.61	1
Cattle, butchered fat	0.04	0.0024	1
Preparation of beef	0.4	0.61	1
Pig meat	0.7	0.88	1
Offal of pigs, edible	0.12	0.12	1
Fat of pigs	0.06	0.006	1
Pork	0.49	0.88	1
Bacon and ham	0.49	0.88	1
Pig, butchered fat	0.06	0.006	1
Pork sausages	0.49	0.88	1
Prepared pig meat	0.49	0.88	1
Lard	0.06	0.006	1
Chicken meat	0.53	0.95	1
Offal and liver of chicken	0.022	0.014	1
Fat liver prepared (foie gras)	0.022	0.014	1
Chicken meat canned	0.53	0.95	1
Fat of poultry	0.022	0.013	1
Fat of poultry, rendered	0.022	0.013	1

[a]Modified from *Hanasaki et al.* [2010].

Blue water evapotranspiration was further subdivided into three categories on the basis of the water source: streamflow, medium-size reservoir, and nonrenewable and nonlocal water.

[11] The virtual water content of unprocessed crop commodities (dimensionless) is calculated as

$$\mathrm{VWC}_{e,c,s} = \frac{\overline{\mathrm{ET}}_{e,c,s}}{Y_{e,c}}, \tag{1}$$

where $\overline{\mathrm{ET}}$ is the evapotranspiration during a cropping period (kg water m^{-2}) and Y is the crop yield (kg crop m^{-2}). The subscripts e, c, and s denote the exporting country, crop, and water withdrawal source, respectively. To transform the VWC of raw crops into that of a processed commodity, (1) is multiplied by $p_x c_x / r_x$. The price ratio (p) is the ratio between the price of the raw crop and the commodity produced from that raw crop. The content ratio (c) indicates the fraction of crop origin ingredients in unit commodities. The yield ratio (r) quantifies the fraction of ingredients in raw crops. Values of r, p, and c are specific to commodity x (r, p, and c for each of the 58 commodities are provided in Table 1, originally provided by *Hanasaki et al.* [2010]). Although crop yield was an output of the H08 model, data from the FAO (FAOSTAT, 2010) was used for increased reliability in the calculation of VWC.

[12] The VWC of unprocessed livestock products (dimensionless) is calculated as

$$\mathrm{VWC}_{e,l,s} = \frac{\mathrm{WC}_{e,l,s}}{P_{e,l}}, \tag{2}$$

where WC is the water consumption per head of livestock (kg water $head^{-1}$) and P is the livestock production per head (kg livestock $head^{-1}$). The subscripts e, l, and s denote the exporting country, livestock product, and water withdrawal source, respectively. To transform the VWC of unprocessed livestock products into that of a processed commodity, (2) is multiplied by $p_x c_x / r_x$. The coefficients p, c, and r have the same meaning as they do for the crop coefficients, and their values for livestock commodities can be found in Table 1. WC was calculated by estimating the virtual water content of livestock feed. Next, the required livestock feed per head was estimated taking into account the life cycle of livestock. Then water use other than feed, such as drinking and cleaning water, was added.

[13] Graphs of the mean VWC are shown in Figure 1. The mean VWC for each of the six world regions (United Nations, Composition of macro geographical (continental) regions, 2010, http://unstats.un.org/unsd/methods/m49/m49regin.htm, hereinafter referred to as United Nations, 2010) is illustrated in Figure 1a, separated into livestock and crop categories. The globally averaged VWC for each of the unprocessed livestock and crop products is provided in Figure 1b.

2.2. Food Trade Data

[14] International food trade statistics list 58 commodities (shown in Table 1) that contain barley, corn, rice, soy, wheat, beef, chicken, or pork. The annual trade matrix (T) of these 58 commodities was obtained from the FAO (FAOSTAT, 2010) for 233 nations in the year 2000. For any discrepancy in the trade volume reported between two nations, the average was taken, with the exception of cases in which no trade was reported by one of the nations, for which we use the reported trade values. When no data were

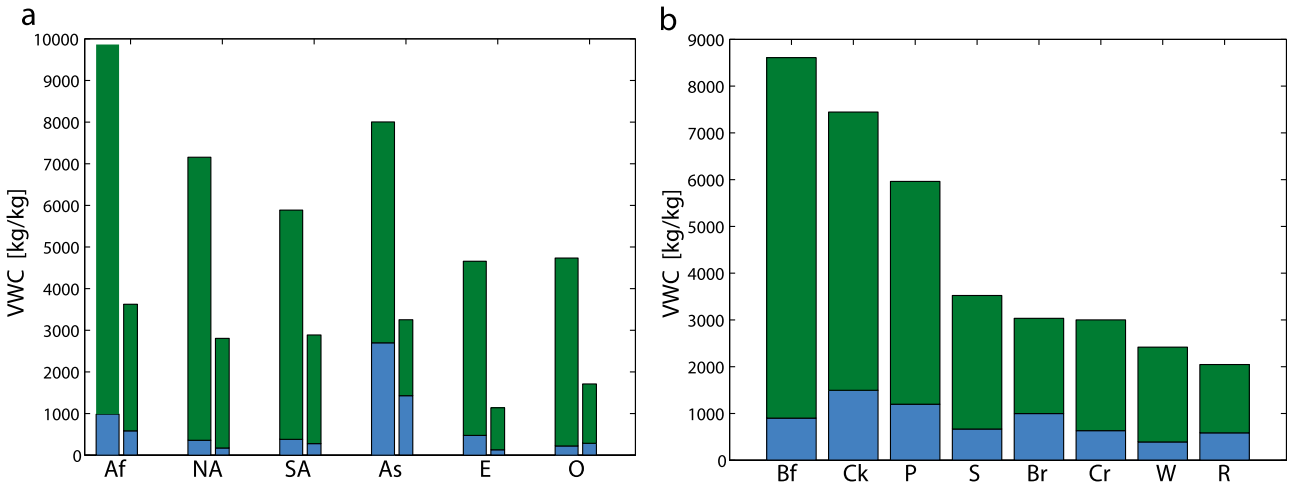

Figure 1. Mean virtual water content (VWC) by water source. The blue portion of the bar represents the blue VWC; the green portion shows the green VWC. (a) Mean VWC for each of the six regions: Africa (Af), North America (NA), South America (SA), Asia (As), Europe (E), and Oceania (O). The thick bars represent the mean VWC for the livestock products: beef, pork, and poultry. The thin bars show the mean VWC for the crops: barley, corn, rice, soy, and wheat. (b) Global average VWC for each of the unprocessed livestock and crop products: beef (Bf), chicken (Ck), pork (P), soy (S), barley (Br), corn (Cr), wheat (W), and rice (R).

reported between two nations, we assumed that no trade occurred between those two nations.

2.3. Network Construction

[15] The VWC and T data in combination allow us to construct the global virtual water trade network (W). In this network, each nation is expressed as a node, and the links represent the volume of virtual water flow between nations. We calculate the virtual water flows between nations by multiplying the crop and livestock trade between nations by the VWC of that crop or livestock product in the country of export. The network connections are thus determined by the agricultural trade relationships and the weight of each connection by the volume of virtual water embodied in the crop and livestock trade.

[16] The total virtual water trade is thus expressed as

$$W_{e,i} = \sum_{s,c} \mathrm{VWC}_{e,a,s} \left[\sum_{x \in a} \frac{p_x c_x}{r_x} T_{e,i,x} \right], \qquad (3)$$

where the subscripts a, x, e, i, and s denote the raw agricultural item (i.e., the raw crop or livestock item), commodity, exporting country, importing country, and water withdrawal source, respectively. The notation $x \in a$ indicates the ensemble of commodities that are produced from the raw agricultural item a. $T_{e,i,x}$ is the annual trade of commodity x from exporting country e to importing country i. W is the virtual water trade between nations ($m^3\ yr^{-1}$) aggregated over all commodities considered in the international food trade. For this reason, we will refer to W as the "aggregate" network throughout this paper, as opposed to a particular commodity or combination of commodities.

[17] The virtual water trade network forms a weighted, directed network, which we will refer to as W_D throughout the rest of this paper to stress the trade direction. Each country involved in trade is a node in the network. A link exists between two nodes that trade with one another. Each link is directed on the basis of the trade flow direction and is weighted by the volume of virtual water. A network map is provided in Figure 2. For any pair of nodes (i, j) the matrix element $W_D(i, j)$ represents the volume of water traded from node i to node j (i.e., node i exports to node j). Note that W_D is not symmetric and $W(i, i) = 0$; that is, a country cannot trade with itself. In the FAO trade data there was one instance, the case of Venezuela, of a country reporting trade with itself. We determined that this data point was erroneous and set it equal to zero.

[18] From the complete network with information on link weights and direction, we create simpler networks: the weighted, undirected network (W_U); the unweighted, directed network (A_D); and the unweighted, undirected network (A_U). An unweighted network is referred to as an adjacency matrix (A). We create these simpler networks to assess network topology with and without link weights and direction. First, W_U was created by symmetrizing the directed, weighted network on the basis of the sum of the link weights between two nodes. This symmetrization creates an undirected network with at most a single link between any two nodes; in W_D and A_D there may be zero, one, or two links between any two nodes. For example, if Japan exports to the United States and the United States exports to Japan in the directed network, there are two links between the nodes representing Japan and the United States. In the undirected networks, these two links are collapsed into a single link. This single link now represents the sum of the volumes of the two former links. Second, A_D and A_U were constructed by replacing all strictly positive elements of W_D and W_U with a unit value.

3. Network Analysis

3.1. Regional Networks

[19] To quantify and visualize flows between world regions, we construct regional virtual water trade networks.

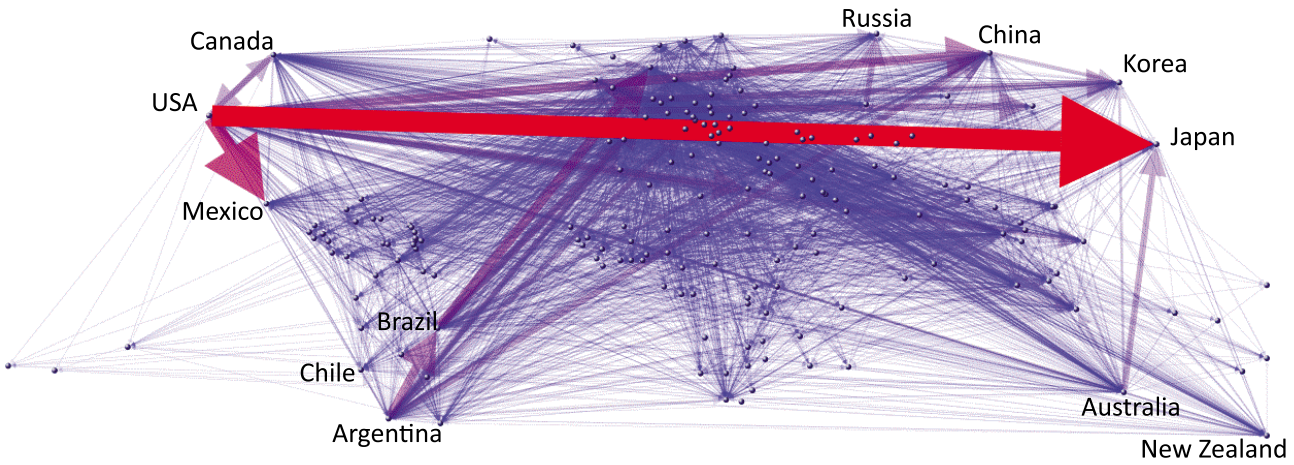

Figure 2. Map of the weighted and directed global virtual water trade network. Each point indicates a node, or nation, in the network. Bilateral trade between countries is displayed by a line between points, with an arrow indicating the direction of trade. The color and width of each line is scaled on the basis of the weight of the link it is representing. In this network, there are 166 nations that import, 151 nations that export, and 6033 links. Note that the export of virtual water from the United States to Japan is the largest link in the network, with a volume of 29.2×10^9 m^3 yr^{-1}, which accounts for approximately 5% of the entire volume in the network. The second largest link is that from the United States to Mexico, with a virtual water trade volume of 20.2×10^9 m^3 yr^{-1}, or approximately 3% of the flow volume.

To do this, we aggregated the virtual water flow at the country scale to the regional scale using the United Nations global regions (United Nations, 2010). We construct nine regional networks on the basis of categories of water source (i.e., green, blue, or total water) and product type (i.e., crop or livestock or both). We used network visualization software [*Krzywinski*, 2009] to create Figure 3. In Figure 3 the links have the same color as their region of origin, and the link width is proportional to the volume of water exchanged. For each region, we have also included the internal trade (i.e., trade between countries of that region). This is represented by links that originate and terminate in the same region. Trade between regions of a negligible size has been excluded from Figure 3 for clarity.

[20] For the aggregate network from all water sources (e.g., Figure 3a), Asia, Europe, and Africa are net importers, while Oceania, North America, and South America are net exporters. The largest link is the export from North America to Asia (over 94×10^9 m^3 yr^{-1}, almost 50% of the total export volume from North America), followed by the export from South America to Europe and Asia (71×10^9 m^3 yr^{-1} and 50×10^9 m^3 yr^{-1}, respectively). Asia is the largest importer of virtual water (267×10^9 m^3 yr^{-1}) and exhibits a large internal trade (77% of exports are internal; refer to Figure 3a). Although Europe imports only 137×10^9 m^3 yr^{-1}, it is the largest importer on a per capita basis, importing 0.34×10^9 m^3 yr^{-1} per capita.

[21] Asia transfers very large amounts of blue water from both crop and livestock products internally (see Figures 3g–3i); about 76% of blue water exports are internal in Asia. On the other hand, South America exports much more green water than blue water. This difference is related to the varying values of blue VWC for both crop and livestock products between these two continents (refer to Figure 1). Livestock and crop commodities produced in Asia utilize much higher values of blue water (33% and 44% of total virtual water content, respectively), while livestock and crop commodities produced in South America use much less blue water (6% and 10% of total virtual water content, respectively). With the exception of North America and Oceania, most of the blue water trade (e.g., Figures 3g–3i) is internal. Note that regions with low VWC import less virtual water from other regions than do regions with high virtual water content. VWC is essentially a measure of how efficient, in terms of water use, because of both climate (i.e., total evapotranspiration) and farming practices (i.e., crop yield), a country or region is in producing a given crop or livestock product. For this reason, it makes sense that regions with a relatively high VWC (i.e., less efficient) import from regions with a comparative advantage in water use (i.e., more efficient).

[22] From Figure 3 we notice that a regional network associated with the crop trade alone drives the aggregate (i.e., both crop and livestock commodities) regional trade network. Note that Figures 3a and 3b are very similar in both link connectivity and magnitude, while Figures 3c and 3d show differences when compared with Figure 3a. Thus, even though the VWC of livestock products is higher than the VWC of crop products (refer to Figure 1), the crop commodity trade drives the aggregated virtual water trade because of the fact that the volumes of crop commodities traded are much larger than volumes of livestock commodities. In fact, the regional crop trade network from green water (e.g., Figure 3e) drives the entire crop trade network (notice the similarities between Figures 3e and 3b, as well as those between Figures 3e and 3a), indicating that this regional network forms the foundation of the aggregate network from all water sources. This highlights the importance of the underlying commodity trade network in driving the virtual water trade considered.

3.2. Undirected Networks

[23] In this section, we will focus our analysis on the symmetric, undirected networks, A_U and W_U. In these networks there are 184 active nodes (nations) and 4550

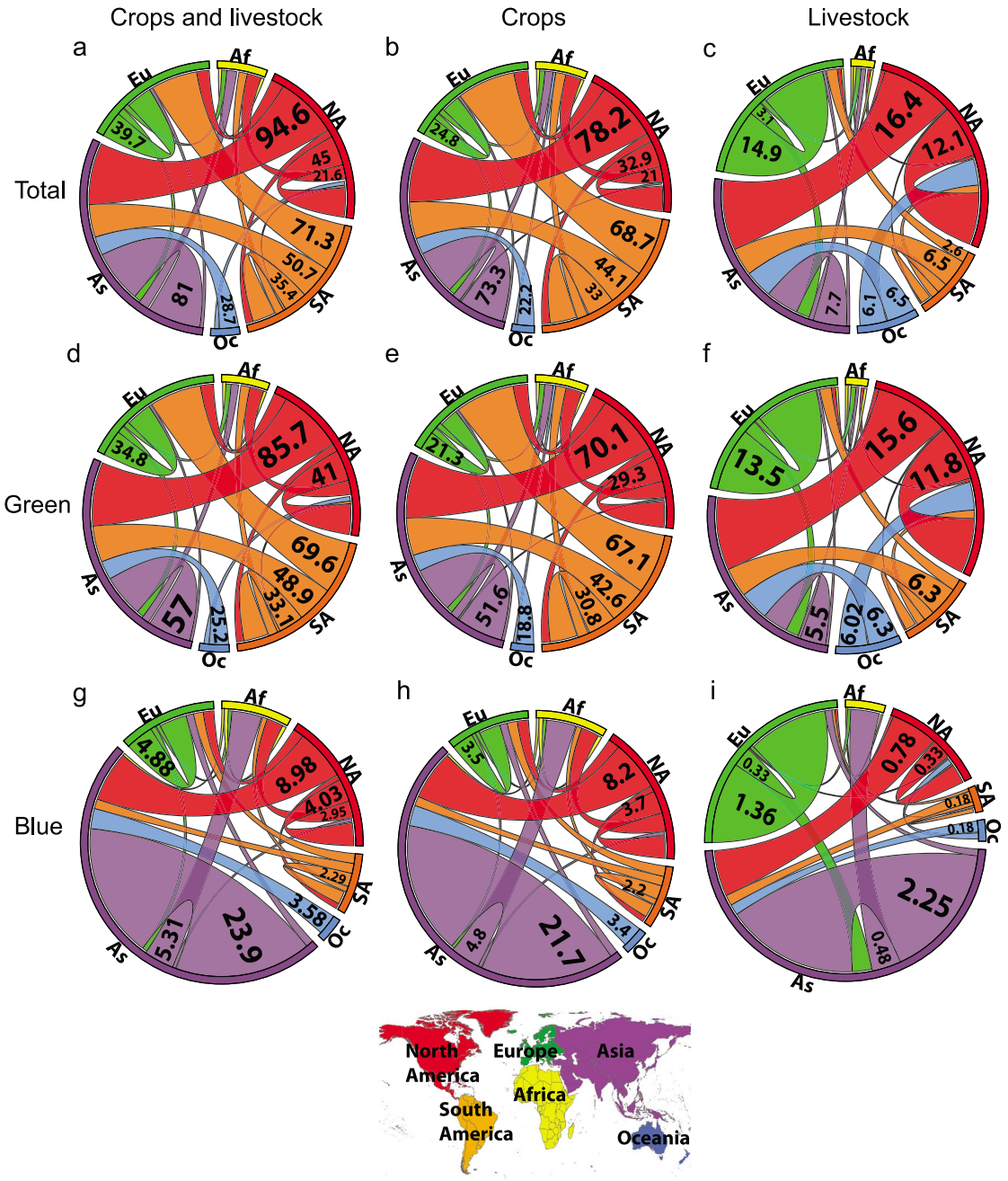

Figure 3. Regional virtual water trade networks. Numbers are in billions of cubic meters of water per year. The regional networks are broken down by source of virtual water and commodity trade. Regional network of virtual water trade from (a) all sources of virtual water associated with trade in both crop and livestock commodities, (b) all sources of virtual water associated with trade in crop commodities only, (c) all sources of virtual water associated with trade in livestock commodities only, (d) green sources of virtual water associated with trade in both crop and livestock commodities, (e) green sources of virtual water associated with trade in crop commodities only, (f) green sources of virtual water associated with trade in livestock commodities only, (g) blue sources of virtual water associated with trade in both crop and livestock commodities, (h) blue sources of virtual water associated with trade in crop commodities only, and (i) blue sources of virtual water associated with trade in livestock commodities only. The regional map at the bottom provides a key to the color scheme of the regional trade networks. Note that the regional acronyms follow those provided in the caption of Figure 1.

links. Element (i, j) of the adjacency matrix, A, is represented by $a_{i,j}$. The elements of the principal diagonal $(a_{i,i})$ are set to 0 and elements off the principal diagonal $(a_{i,j})$ are equal to 1 when there is flow between nodes i and j. In this symmetric matrix, $a_{i,j} = a_{j,i}$. Similarly, we constructed the symmetric weighted matrix W_U, in which the elements $w_{i,j}$ are computed as the sum of the $i \rightarrow j$ and $j \rightarrow i$ flows between the corresponding nations.

Table 2. Country Rankings in 2000[a]

	Undirected		Export		Import	
Rank	k	Country	k_{out}	Country	k_{in}	Country
1	162	Netherlands	159	United States	97	United States
2	162	United States	158	Netherlands	94	UK
3	161	France	154	France	89	Germany
4	156	UK	152	Italy	87	Canada
5	154	Italy	150	UK	84	Netherlands
6	152	Germany	149	Germany	82	France
7	146	Belgium	142	Denmark	72	Saudi Arabia
8	145	China	142	Belgium	69	Japan
9	144	Denmark	142	China	68	Spain
10	141	Canada	136	Canada	68	Belgium
11	133	Australia	129	Thailand	67	Switzerland
12	133	Thailand	126	Australia	65	Italy
13	126	Spain	124	Argentina	64	Australia
14	125	Argentina	124	Brazil	64	Russia
15	125	Brazil	119	Spain	60	Hong Kong

[a]Top 15 positions according to node degree (k) statistics. Node degree is a measure of the number of trade partners of a given country, k is a measure of the trade connections in the undirected network, k_{out} counts the number of export trade partners, and k_{in} counts the number of import trade partners.

[24] A fundamental network property is the node degree (k), which measures the number of links of each node and is defined as $k_i = \Sigma_j a_{i,j}$. Here the node degree is a measure of the number of trade partners of each nation. Node degree values range from 1 to 162, with an average value of $\langle k \rangle$ = 49.46. The node degree is a first approximation of its topological centrality, which is an indication of its importance within the network. Two nations share the maximum node degree value of 162: Netherlands and the United States (see Table 2 for a ranking of the top 15 nations in terms of node degree). Node degree statistics for the aggregate and individual crop networks are collected in Table 3.

[25] The volume of water traded globally is 625×10^9 m^3 yr^{-1} (calculated as $1/2\Sigma_{i,j} w_{i,j}$). The link weights range from 77.72 m^3 yr^{-1} to 29.2×10^9 m^3 yr^{-1} with a mean value of $\langle w \rangle = 137 \times 10^6$ m^3 yr^{-1}, indicative of high link weight heterogeneity. The largest link in this network is between the United States and Japan, with a virtual water trade of 29.2×10^9 m^3 yr^{-1}, which accounts for 4.7% of the entire volume in the network. The second largest link is that between the United States and Mexico, with a virtual water trade volume of 20.2×10^9 m^3 yr^{-1}, or 3.2% of the flow volume. In fact, in W_U the United States is involved in 7 out of the 10 largest links (refer to Table 4).

[26] Node strength (s) is a measure of the weight of each node's links. This value is calculated as $s_i = \Sigma_j w_{i,j}$. Node strength values range from 50×10^3 to 183×10^9 m^3 yr^{-1}, with an average value of 6.79×10^9 m^3 yr^{-1}. The nation that trades the most virtual water (i.e., maximum strength) is the United States. Refer to Table 5 for the top 15 ranked nations in terms of the volume of virtual water traded. This node strength information provides a description of the centrality of nations according to the volume of virtual water traded.

[27] Graphs of undirected network properties are provided in Figure 4. The cumulative degree distribution $P(K > k)$ is shown in Figure 4a. Many empirical analyses of real-world networks in the literature fit a power law to the tail of $P(K > k)$ [e.g., *Barrat et al.*, 2004; *Garlaschelli and Loffredo*, 2005; *Kyriakopoulos et al.*, 2009]. However, it is clear that here the simple exponential distribution, e.g., $P(K > x) = e^{-\lambda x}$, as used by *DeMontis et al.* [2007], accurately reflects the entirety of the data set (an exponential distribution of $\langle k \rangle$ is shown by the solid line in Figure 4a). Thus, the topology of the food trade networks exhibits a characteristic scale, different from the scale-free behavior of other real-world systems, such as those highlighted by *Barabási and Albert* [1997]. The exponential parameter is given by $\langle k \rangle$ and is provided for each individual crop network in Table 3.

[28] The cumulative distribution of node strength is shown in Figure 4b, where a stretched exponential distribution, e.g., $P(K > x) = e^{(-\lambda x)^{\alpha}}$, is compared with the data. The stretched exponential distribution parameter (α) for the aggregate and individual crop networks is provided in Table 3. This fat-tailed distribution indicates that the volumes of virtual water traded by each nation are highly heterogeneous. Thus, when the network weights are considered, a heavy-tailed distribution is required to fit the data, unlike the exponential distribution fit to the node degrees. This implies that the inclusion of network weights increases the heterogeneity of the system in a nontrivial way.

[29] Probability distributions are frequently used in the natural sciences to explain data. Many environmental variables are distinctly asymmetric (i.e., non-Gaussian) and

Table 3. Global Network Measures for Undirected Virtual Water Trade Networks

		Crop								
	Symbol	Barley	Corn	Rice	Soy	Wheat	Beef	Pork	Poultry	Aggregate
Active nodes	N	175	178	175	175	178	172	169	168	184
Global flow (m^3 yr^{-1})	g	30.5×10^9	62.9×10^9	52.9×10^9	241×10^9	137×10^9	59.2×10^9	19.7×10^9	21.6×10^9	625×10^9
Number of links	L	2257	1633	1860	1712	2664	1835	1675	1466	4550
Average degree	$\langle k \rangle$	25.79	18.35	21.23	19.57	29.93	21.34	19.82	17.45	49.46
Maximum degree	$k^{\max}$	148	141	135	123	150	111	118	134	162
Average strength (m^3 yr^{-1})	$\langle s \rangle$	0.35×10^9	0.71×10^9	0.61×10^9	2.75×10^9	1.54×10^9	0.69×10^9	0.23×10^9	0.26×10^9	6.79×10^9
Maximum strength (m^3 yr^{-1})	$s^{\max}$	7.23×10^9	30.9×10^9	17.0×10^9	67.4×10^9	39.6×10^9	23.4×10^9	6.31×10^9	8.38×10^9	183×10^9
Clustering coefficient	c	0.71	0.62	0.62	0.67	0.69	0.64	0.73	0.68	0.75
Clustering coefficient random	c_{ER}	0.15	0.10	0.12	0.11	0.17	0.12	0.12	0.10	0.27
Clustering coefficient weighted	c^W	0.79	0.73	0.73	0.77	0.80	0.73	0.80	0.79	0.87
Stretched exponential parameter	γ	0.28	0.22	0.22	0.2	0.24	0.35	0.3	0.24	0.28

Table 4. Link Rankings in 2000[a]

Rank	$w_U(i, j)$ (m^3 yr^{-1})	Country 1	Country 2	$w_D(i, j)$ (m^3 yr^{-1})	Country of Export	Country of Import
1	29.2×10^9	United States	Japan	29.2×10^9	United States	Japan
2	20.2×10^9	United States	Mexico	19.2×10^9	United States	Mexico
3	14.5×10^9	Canada	United States	12.9×10^9	Brazil	Netherlands
4	12.9×10^9	Brazil	Netherlands	12.0×10^9	United States	China
5	12.5×10^9	Argentina	Brazil	11.9×10^9	Argentina	Brazil
6	12.0×10^9	United States	China	9.17×10^9	United States	Egypt
7	9.17×10^9	United States	Egypt	8.84×10^9	Brazil	France
8	8.90×10^9	Brazil	France	8.65×10^9	United States	Taiwan
9	8.65×10^9	United States	Taiwan	8.30×10^9	Argentina	China
10	8.30×10^9	United States	Korea	8.28×10^9	United States	Korea
11	8.30×10^9	Argentina	China	8.08×10^9	Canada	United States
12	7.79×10^9	Australia	Japan	7.79×10^9	Australia	Japan
13	7.68×10^9	Kazakhstan	Russia	7.61×10^9	Kazakhstan	Russia
14	7.49×10^9	Argentina	Spain	7.48×10^9	Argentina	Spain
15	6.88×10^9	Argentina	Italy	6.87×10^9	Argentina	Italy

[a]Top 15 positions according to link weight (w): $w_U(i, j)$ represents element (i, j) in the weighted, undirected network and W_D(i, j) represents element (i, j) in the weighted, directed network. Note that we report which two countries share a particular link for $w_U(i, j)$. Since there is no direction in this network the import-export relationship does not exist.

important to properly quantify. For example, the Gamma distribution has been often used to explain precipitation data, with important applications in hydrologic models, such as flooding or drought estimates [*Wilks*, 2006]. Similarly, we believe that the distributions of virtual water resources presented here, influenced by both social and natural forces, provide necessary statistical descriptions of the linked water and food system for water resource professionals.

[30] To explore in further detail the relationship between the node connectivity and weights, we plot the strength of the nodes as a function of their degree in Figure 4c. We observe a power law relationship that follows the form $s(k) \sim k^{\beta}$. The parameter $\beta = 2.60$ for the aggregate network and is provided in Table 6 for the individual crop networks. This high β value indicates that there is a strong relationship between the volume of virtual water that each nation trades and its number of trade partners. The node strength grows faster than node degree, so the more trade connections a country has, the much more it is able to participate in the exchange of virtual water in a highly nonlinear way.

[31] While node degree is the simplest proxy for centrality, it is a local measure that does not provide any information about the importance of the node within the global structure [*Barthelemy*, 2004]. A measure of centrality that takes into account the location of a node within the entire network architecture is the betweenness centrality, which counts the fraction of shortest paths going through a given node. The betweenness centrality (B) is defined as $B_u = \Sigma_{i,j} \frac{\sigma(i,u,j)}{\sigma(i,j)}$, where $\sigma(i, u, j)$ is the number of shortest paths between nodes i and j that pass through node u, $\sigma(i, j)$ is the total number of shortest paths between i and j, and the sum is over all pairs i, j of nodes [*Costa et al.*, 2007]. We normalize B by $(N - 1)(N - 2)/2$ to maintain $B \in [0, 1]$ as suggested by *Barthelemy* [2004].

[32] B is an important measure of how important a node is in terms of connecting other nodes in the network [*Jackson*, 2008]. The United States has the highest betweenness centrality in the virtual water trade network, as shown in Table 7, highlighting its crucial role in the global structure. France and the United Kingdom also exhibit high betweenness centrality, ranking a close second and third,

Table 5. Country Rankings in 2000[a]

	Undirected		Export		Import		Import per Capita	
Rank	s (m^3 yr^{-1})	Country	s_{out} (m^3 yr^{-1})	Country	s_{in} (m^3 yr^{-1})	Country	s_{in} ($capita^{-1}$)	Country
1	183×10^9	United States	165×10^9	United States	52.1×10^9	Japan	1,954	United Arab Emirates
2	92.7×10^9	Argentina	91.0×10^9	Argentina	31.1×10^9	China	1,885	Aruba
3	88.2×10^9	Brazil	69.7×10^9	Brazil	28.7×10^9	Netherlands	1,802	Netherlands
4	52.5×10^9	Japan	38.5×10^9	Australia	24.2×10^9	Korea	1,375	Cyprus
5	44.5×10^9	China	34.5×10^9	India	21.8×10^9	Mexico	1,242	Qatar
6	40.7×10^9	Canada	32.7×10^9	Canada	21.8×10^9	Iran	1,158	Singapore
7	39.3×10^9	Australia	20.0×10^9	Thailand	19.5×10^9	Italy	1,153	Hong Kong
8	37.7×10^9	India	18.1×10^9	France	19.3×10^9	Egypt	1,127	Denmark
9	36.8×10^9	Netherlands	13.4×10^9	China	18.8×10^9	Indonesia	1,097	Seychelles
10	35.5×10^9	France	12.7×10^9	Kazakhstan	18.5×10^9	Brazil	974	Kuwait
11	30.0×10^9	Thailand	11.7×10^9	Germany	18.3×10^9	Spain	927	Belgium
12	27.7×10^9	Germany	11.2×10^9	Pakistan	17.6×10^9	Russia	826	Uruguay
13	25.0×10^9	Italy	8.65×10^9	Denmark	17.5×10^9	France	822	Netherlands Antilles
14	24.5×10^9	Korea	8.06×10^9	Netherlands	17.4×10^9	United States	821	Malta
15	24.1×10^9	Mexico	7.35×10^9	Paraguay	16.1×10^9	Germany	801	Israel

[a]Top 15 positions according to node strength (s) statistics. Node strength is a measure of the weight of a given country; s is the volume of virtual water traded by a country in the undirected network, s_{out} measures the volume of virtual water exported by a country, and s_{in} measures the volume of virtual water imported by a country.

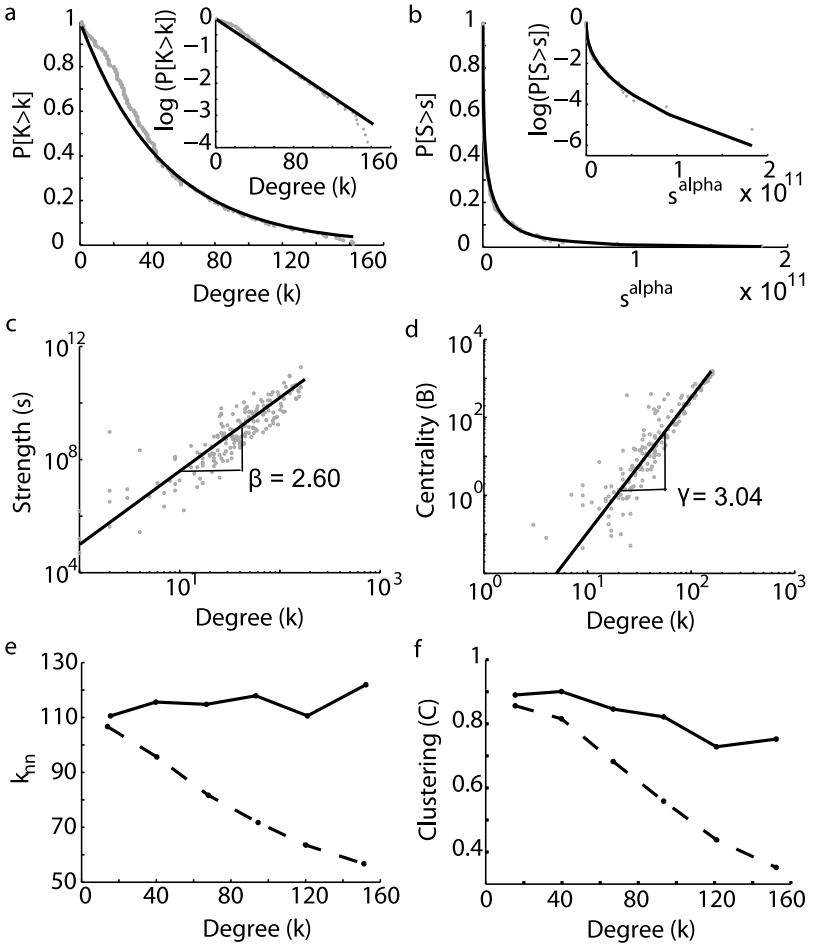

Figure 4. Graphs for the undirected virtual water trade network. (a) The cumulative distribution of the node degrees compared with an exponential distribution of parameter $\langle k \rangle = 49.46$. (b) The cumulative distribution of the node strength compared with a stretched exponential distribution of parameter $\alpha = 0.42$. (c) Node strength plotted against node degree exhibiting a power law relationship of the form $s(k) \sim k^{\beta}$, with parameter $\beta = 2.60$. (d) Betweenness centrality of each node plotted against node degree exhibiting a power law relationship of the form $B(k) \sim k^{\gamma}$, with parameter $\gamma = 3.04$. (e) Weighted (solid line) and unweighted (dashed line) average nearest-neighbor degree as a function of node degree. (f) Weighted (solid line) and unweighted (dashed line) clustering coefficient as a function of node degree.

respectively, with values closely trailing the United States. The United States, France, and the United Kingdom all exhibit B values that are approximately 3 times higher than other highly ranked countries, such as Spain and India (e.g., ranked 14th and 15th out of 184 countries, respectively). B versus node degree follows a power law distribution of the form $B(k) \sim k^{\gamma}$, shown in Figure 4d. The parameter $\gamma = 3.04$ for the aggregate network, and it is provided in Table 6 for individual crop networks.

[33] We next consider the network correlation structure, typically quantified using the average nearest-neighbor degree (k_{nn}); k_{nn} measures the affinity of a given node to connect to high- or low-degree neighbors. The unweighted definition of k_{nn} is given by [*Pastor-Satorras et al.*, 2001]

$$k_{\mathrm{nn}_i} = \frac{1}{k_i} \sum_{j \in V(i)} k_j, \tag{4}$$

where $j \in V(i)$ indicates the j neighbors of node i. Thus, k_{nn_i} identifies all nodes in the neighborhood of i (i.e., connected to node i), sums their respective node degrees, then normalizes by the node degree of node i.

Table 6. Parameters for Each Network

		Crop								
	Symbol	Barley	Corn	Rice	Soy	Wheat	Beef	Pork	Poultry	Aggregate
s versus k	β	2.37	2.28	1.87	2.68	2.15	2.41	2.41	2.07	2.60
s_{in} versus k_{in}	β_{in}	2.16	2.71	2.02	3.32	2.12	2.63	2.75	2.20	3.05
s_{out} versus k_{out}	β_{out}	2.21	1.71	1.76	1.90	1.75	2.10	1.91	1.91	1.93
B versus k	γ	2.76	2.58	2.61	2.60	2.70	2.56	2.79	2.31	3.04

Table 7. Country Rankings in 2000[a]

Rank	*B*	Country
1	0.093	United States
2	0.092	France
3	0.091	United Kingdom
4	0.078	Netherlands
5	0.068	Italy
6	0.065	Germany
7	0.063	China
8	0.053	Denmark
9	0.052	Australia
10	0.049	Canada
11	0.045	Thailand
12	0.044	Japan
13	0.038	South Africa
14	0.034	Spain
15	0.032	India

[a]Top 15 positions according to node betweenness centrality (*B*) statistics. Node betweenness centrality measures the centrality of each node in terms of its location within the global network architecture.

[34] The behavior of k_{nn} as a function of k allows us to determine whether or not the network exhibits degree correlations. If k_{nn} increases with k, the network is referred to as assortative, and nodes with a high degree tend to connect to other nodes with a high degree, while nodes with a low degree tend to connect to nodes with a low degree. However, if k_{nn} is a decreasing function of k, then the network is disassortative, indicating that nodes of high degree tend to connect to neighbors with low degree and nodes of low degree tend to connect to others with a high degree. In Figure 4e, we see that for the undirected case, k_{nn} decreases with k, suggesting that the global virtual water trade network is disassortative, typical of technological, biological, and transportation networks [*Newman*, 2003; *Costa et al.*, 2007]. In other words, when we consider only network topology, nations of high degree tend to be connected to nations that have a low degree. This disassortative behavior indicates that the network exhibits a global architecture in which hubs (i.e., nations with high degree) provide the connectivity for the peripheral nations with small degree [*DeMontis et al.*, 2007].

[35] The definition of k_{nn} has been extended for weighted networks by [*Barrat et al.*, 2004]

$$k^W_{\mathrm{nn}_i} = \frac{1}{s_i}\sum_{j\in V(i)} w_{ij}k_j, \tag{5}$$

where, as in the unweighted definition, $j \in V(i)$ indicates the j neighbors of node i. The value of the links between node i and its neighbors (w_{ij}) is now accounted for, in addition to the node degree of the neighbors, before normalizing by the node strength of i rather than the node degree of i as in the unweighted definition. This definition measures the affinity of a node to connect with low- or high-degree neighbors on the basis of the magnitude of the actual interactions. If links with large edges point to neighbors with large degree, then $k^W_{nn}(k) > k_{nn}(k)$. However, $k^W_{nn}(k) < k_{nn}$ if links with large weights point to neighbors with low degree [*Barrat et al.*, 2004].

[36] Both k_{nn} and k^W_{nn} are plotted against k in Figure 4e. Note that the disassortative structure of the unweighted k_{nn} breaks down when weights are taken into account (compare the solid line with the dashed line in Figure 4e). The difference between k^W_{nn} and k_{nn} grows with increasing k, indicating that highly connected nations are more likely to be connected when link flows are considered. In sharp contrast to topological disassortativity, we observe an affinity between nations of high degree which exchange large volumes of virtual water. In other words, large weights preferentially connect hubs, while nodes of a smaller degree are connected via smaller weights.

[37] The clustering coefficient allows us to study the tendency of nations in the network to form tightly connected groups. The clustering coefficient is defined as

$$c_i = \frac{2e_i}{k_i(k_i-1)}, \tag{6}$$

where e_i is the number of links between the k_i neighbors of node i and $k_i(k_i - 1)/2$ is the maximum possible number of links existing between the k_i neighbors of i [*Boguna and Pastor-Satorras*,2003; *DeMontis et al.*, 2007]. In other words, c_i counts the number of closed triangles formed in the neighborhood of node i. This value measures the local cohesiveness of the network and $\in$ [0,1]. Values of $c_i = 0$ indicate that the neighbors of i are not connected at all, while values of $c_i = 1$ correspond to the case in which all the neighbors of i are themselves connected. The average clustering coefficient of the virtual water trade network is 0.75, much higher than that of a random network (c_{ER}) with the same number of links and nodes (refer to Table 3; $c_{ER} = 0.27$), where $c_{ER} = L/N(N-1)$ [*Bollobás*, 1985].

[38] The definition of c_i has been extended to weighted networks by *Barrat et al.* [2004] and is defined as

$$c^W_i = \frac{1}{s_i(k_i-1)}\sum_{j,h}\frac{(w_{ij}+w_{ih})}{2}a_{ij}a_{ih}a_{jh}, \tag{7}$$

where $1/s_i(k_i - 1)$ is a normalization factor to maintain $c^W_i \in$ [0,1]. Using this definition, the relative weight of closed triangles in the neighborhood of node i is considered. Here the mean weighted clustering coefficient is greater than the unweighted version (refer to Table 3; $c^W = 0.87 > c = 0.75$), indicating that cohesiveness is more likely when link weights are taken into account.

[39] We plot c and c^W as a function of node degree in Figure 4f; c decreases with increasing values of k. This behavior indicates that nations with a low degree belong to tightly connected groups of nations, while nations with high degree connect otherwise disconnected portions of the network [*DeMontis et al.*, 2007]. Here, as with the nearest-neighbor degree, the introduction of network weights destroys the correlation structure, such that $c^W(k)$ is approximately constant and $c^W(k) > c(k)$ over the whole range of degrees.

[40] In summary, the disassortative behavior of the average nearest-neighbor degree and the clustering coefficient breaks down with the inclusion of network weights (refer to Figures 4e and 4f). The accumulation of weight on highly connected nations destroys the disassortative behavior, suggesting the existence of the "weighted rich club" phenomenon [*DeMontis et al.*, 2007]. This phenomenon occurs when prominent elements in a system engage in stronger or weaker interactions among themselves than expected by pure chance [*Opsahl et al.*, 2008]. Thus, when we utilize

information on the volume of virtual water embedded in each trade link, we obtain additional insights into the network organizing principles.

3.3. Directed Networks

[41] We now consider the direction of trade in the network analysis. In this section we focus our attention on the A_D and W_D networks. Direction is an important characteristic because the virtual water trade network is not symmetric, which means that information on the network structure is lost when we symmetrize the network for the undirected analysis. In these directed networks there are 151 nations that export, 166 nations that import, and 6033 links. There are some nations that either import or export but not both (e.g., Qatar does not export but only imports). The global volume of water traded in the directed network is equivalent to that of the undirected network at 625×10^9 m^3 yr^{-1}. Our global flow volume is slightly greater than that found by *Hanasaki et al.* [2010] (i.e., 625×10^9 m^3 yr^{-1} compared with 545×10^9 m^3 yr^{-1}) because of the fact that we utilize both the import and export trade data from the FAO.

[42] As in the undirected case, $a_{i,j}$ represents element i, j of the adjacency matrix. The elements of the principal diagonal ($a_{i,i}$) are set to 0 and elements off the principal diagonal ($a_{i,j}$) are equal to 1 when there is flow $i \rightarrow j$. However, unlike in the symmetric case, element $a_{i,j} \neq a_{j,i}$. In the weighted matrix (W_U), the elements ($w_{i,j}$) represent the flows $i \rightarrow j$ between the corresponding nations. Note that $w_{i,j}$ is no longer equivalent to $w_{j,i}$.

[43] We now consider the out- and in-node degrees, which provide additional information on the heterogeneity of the network connectivity. The out-node degree ($k_{\text{out}_i} = \Sigma_j\, a_{i,j}$) values range from 0 to 159 with a mean value of 32.79; the in-node degree ($k_{\text{in}_i} = \Sigma_j\, a_{j,i}$) values range from 0 to 97 with a mean value of 32.79. We rank each nation according to its degree for both the undirected and directed network in Table 2. Note that the United States has the highest k_{in} and k_{out} values. This is striking, since Netherlands and the United States tie for the highest rank in the undirected network. This indicates that although the United States has the most import and export trading partners, there is significant overlap in these trading partners such that when A_D is symmetrized, Netherlands gains the most links. Netherlands is a strategic harbor in Europe, so this diversity in trading partners makes sense.

[44] The cumulative distributions of the out- and in-node degrees of A_D are shown in Figures 5a and 5b. We compare an exponential distribution of parameter $\langle k_{\text{out}} \rangle$ to the out-node degrees and parameter $\langle k_{\text{in}} \rangle$ to the in-node degrees, as we did for the undirected network. Note that the in-node degree does not follow an exponential distribution, while the out-node degree distribution does appear to follow an exponential. The tail of k_{out} is fatter than the tail of k_{in}. The tail of k_{in} actually drops off quicker than an exponential distribution (refer to the tails in Figures 5a and 5b). This indicates that it is frequent that countries will export to many trade partners, while they tend to import from just a few trade partners. This makes sense, since if a country is efficient at producing a given commodity, then it will likely export it to many partners. However, if a nation must import a given commodity, it will likely be able to meet its demand for this commodity in a few trade relationships.

[45] The link weights in the directed network range from 77.72 m^3 yr^{-1} to 29.2×10^9 m^3 yr^{-1}, with a mean value of 104×10^6 m^3 yr^{-1}. The largest link weight in W_D is United States → Japan, with a value of 29.2×10^9 m^3 yr^{-1}, or 4.7% of the network's total flow. The United States and Japan have been shown to be important nations in the virtual water literature [*Hoekstra and Hung*, 2005; *Hoekstra and Chapagain*, 2008], which this study confirms. The second largest link in the network is United States → Mexico, with a value of 20.2×10^9 m^3 yr^{-1}, which represents 3.1% of the global flow. Even though the links between Japan and the United States and the United States and Mexico were also the largest links in the undirected network, we are now able to distinguish flow direction. The link between Canada and the United States is the third largest link in the symmetric network (with a value of 14.5×10^9 m^3 yr^{-1}) but the 11th largest link in the directed network. In the directed network, the link Canada → United States accounts for 8.08×10^9 m^3 yr^{-1} (see Table 4), a whole order of magnitude less, because of the fact that trade United States → Canada is also relatively large (valued at 6.46×10^9 m^3 yr^{-1}). This example illustrates that information is lost through network symmetrization.

[46] Differences between our virtual water flow volumes and other values reported in the literature can be attributed to differences in VWC and the agricultural commodities considered, though major differences are mainly due to differences in the underlying commodities. For example, we calculate the total virtual water import of the United States due to crop commodities to be 8.21×10^9 m^3 yr^{-1}. However, *Hoekstra and Hung* [2005], whose study is based on 38 crop commodities, determine that the United States imports 29.3×10^9 m^3 yr^{-1}, while *Hoekstra and Chapagain* [2008], in a study based on 285 crop commodities, calculate the same value at 73.1×10^9 m^3 yr^{-1}. It makes sense that we would obtain a much lower value than *Hoekstra and Chapagain* [2008] for the import of crops to the United States, since this wealthy nation likely imports many specialty crops that are not included in our analysis, since we focus on staple crops. Our values compare relatively well for other flows.

[47] For weighted, directed networks the natural generalization of the out and in degree of a node is the out- and in-node strength, where $s_{\text{out}_i} = \Sigma_j\, w_{i,j}$ and $s_{\text{in}_i} = \Sigma_j\, w_{j,i}$, respectively. The import volumes (s_{in}) range from 0 m^3 yr^{-1} to 52.1×10^9 m^3 yr^{-1}, with a mean value of 3.40×10^9 m^3 yr^{-1}; the export volumes (s_{out}) range from 0 m^3 yr^{-1} to 165×10^9 m^3 yr^{-1}, also with a mean value of 3.40×10^9 m^3 yr^{-1}. The cumulative distributions of the in- and out-node strengths are compared with the stretched exponential distribution in Figures 5c and 5d. As in the undirected network, the stretched exponential distribution provides an excellent fit to the directed node strength distributions. This indicates that the high node strength heterogeneity is maintained when direction is taken into account.

[48] We rank nations according to their strength in Table 5. Table 5 provides additional insight into the node strength heterogeneity that is lost by symmetrizing the network to create the undirected network. For example, Japan imports the largest volume of virtual water but ranks 52nd in terms of export volume. However, when we symmetrize the directed network on the basis of the sum of trade between any two nations, we lose this information and Japan becomes the fourth-ranked nation in terms of node strength.

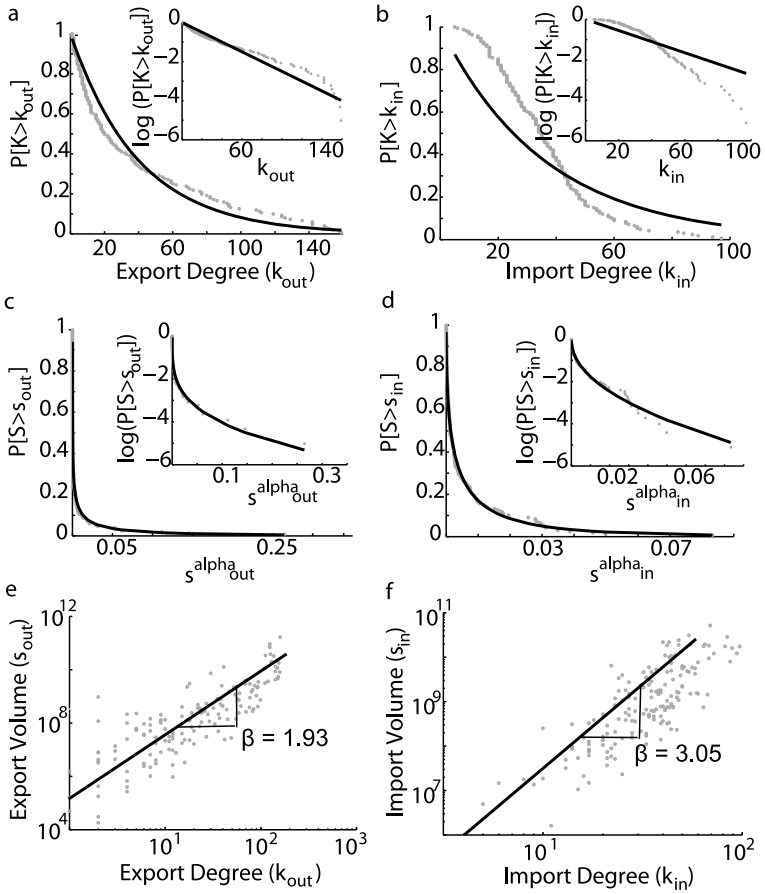

Figure 5. Graphs for the directed virtual water trade network. (a) The cumulative distribution of the out-node degrees compared with an exponential distribution of parameter $\langle k_{out} \rangle = 32.79$. (b) The cumulative distribution of the in-node degrees compared with an exponential distribution of parameter $\langle k_{in} \rangle = 32.79$. (c) The cumulative distribution of the out-node strengths compared with a stretched exponential distribution of parameter $\alpha_{out} = 0.28$. (d) The cumulative distribution of the in-node strengths compared with a stretched exponential distribution of parameter $\alpha_{in} = 0.48$. (e) Out-node strength plotted against out-node degree exhibiting a power law relationship of the form $s_{out}(k_{out}) \sim k_{out}^{\beta out}$, where parameter $\beta_{out} = 1.93$. (f) In-node strength plotted against in-node degree exhibiting a power law relationship of the form $s_{in}(k_{in}) \sim k_{in}^{\beta in}$, where parameter $\beta_{in} = 3.05$.

Similarly, Australia is the fourth largest global exporter of virtual water but comes in 87th in terms of import and 7th in the undirected case. When we analyze the volume of virtual water that each country imports on a per capita basis, the rankings change dramatically. The United Arab Emirates is the largest importer per capita. Most of the nations that import a lot of virtual water on a per capita basis are either island nations or wealthy countries with a relatively small population. Importantly, many of these countries are extremely arid (i.e., United Arab Emirates, Qatar, Kuwait, and Israel) or lack sufficient water and land resources for agricultural production (i.e., Aruba, Cyprus, Singapore, Hong Kong, Seychelles, Netherlands Antilles, and Malta).

[49] As in the undirected network analysis, we plot the strength of the nodes as a function of their degree in Figures 5e and 5f. Similarly, we observe a power law relationship that follows the form $s_{in}(k_{in}) \sim k_{in}^{\beta in}$ and $s_{out}(k_{out}) \sim k_{out}^{\beta out}$. The parameter β_{in} is 3.05, and the parameter β_{out} is 1.94 for the aggregate network and is provided in Table 6 for the individual crop networks. These high β values indicate that the strong relationship between the volume of virtual water and trade connections remains when direction is taken into account. In fact, the value of β_{in} is larger than the value of β, which indicates that the relationship between s_{in} and k_{in} is even stronger than the relationship between the undirected strength and node degree, particularly for the soy network, where $\beta_{in} = 3.32$.

[50] Thus, as nations increase the number of countries that they import from, they increase the volume of virtual water obtained at an even greater rate. This finding has important policy implications, indicating that increasing the number of import trade partners is an efficient way for countries to improve access to water resources. In our related paper [*Suweis et al.*, 2011], we develop a model of global virtual water trade with predictive capabilities, in which we detail the controls on the network structure. We find that both economic and climatologic factors are necessary to capture the global properties. In particular, the gross domestic product of each nation is used to model the connectivity structure, while the rainfall on agricultural area is necessary to determine the weighted network properties (i.e., the volumes of virtual water). Thus, both the economy and

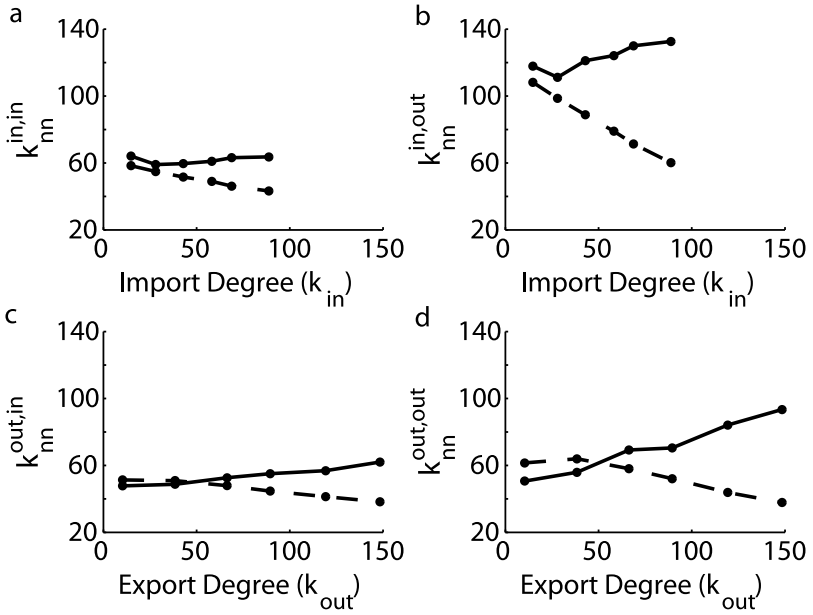

Figure 6. Graphs of the weighted (solid line) and the topological (dashed line) assortativity for the directed network. (a) The import neighbors and their import characteristics (for the unweighted and weighted definition, refer to (8) and (12), respectively). (b) The import neighbors and their export characteristics (for the unweighted and weighted definition, refer to (10) and (14), respectively). (c) The export neighbors and their import characteristics (for the unweighted and weighted definition, refer to (11) and (15), respectively). (d) The export neighbors and their export characteristics (for the unweighted and weighted definition, refer to (9) and (13), respectively). Note that the disassortativity structure exhibited in all of the unweighted networks breaks down when the network weights are considered.

the water resources of a country are necessary to reproduce the network and explain why a country with more trade partners exchanges much more virtual water. Note that our finding that water availability is a determinant of virtual water trade differs from the findings of *Ma et al.* [2006] and *Verma et al.* [2009], who find that water availability does not drive virtual water trade. Please refer to *Suweis et al.* [2011] as we do not go into model details in this paper.

[51] When direction is taken into account, the average nearest-neighbor degree breaks into four classes: $k_{nn}^{out,in}$, $k_{nn}^{out,out}$, $k_{nn}^{in,out}$ and $k_{nn}^{in,in}$. The first element in the superscript determines the neighborhood of node i , while the second element labels the characteristic of the neighbors. For example, $k_{nn_i}^{in,out}$ determines the neighbors that node i imports from and then calculates their export partnerships [*Foster et al.*, 2010]. We perform a local unweighted average of the directed nearest neighbor degrees, defined as

$$k_{nn_i}^{in,in} = \frac{1}{k_{in_i}} \sum_{j \in V_{in_{(i)}}} a_{ji} k_{in_j}, \tag{8}$$

$$k_{nn_i}^{out,out} = \frac{1}{k_{out_i}} \sum_{j \in V_{out_{(i)}}} a_{ij} k_{out_j}, \tag{9}$$

$$k_{nn_i}^{in,out} = \frac{1}{k_{in_i}} \sum_{j \in V_{in_{(i)}}} a_{ji} k_{out_j}, \tag{10}$$

$$k_{nn_i}^{out,in} = \frac{1}{k_{out_i}} \sum_{j \in V_{out_{(i)}}}, a_{ij} k_{in_j} \tag{11}$$

where $j \in V(i)$ indicates the j neighbors of node i for a given trade direction. For example, $\in V_{in_{(i)}}$ indicates the neighbors from which node i imports. Once the appropriate neighborhood of i has been established, then the degree of nodes (again, of a particular direction) within that neighborhood are summed; $1/k_i$ serves as the normalization factor.

[52] We extend the definition of k_{nn}^{W} as given by *Barrat et al.* [2004] for weighted undirected networks and as suggested by *Kyriakopoulos et al.* [2009]. Here we provide the explicit equations for the local weighted average of the directed nearest-neighbor degree:

$$k_{nn_i}^{W(in,in)} = \frac{1}{s_{in_i}} \sum_{j \in V_{in_{(i)}}} w_{ji} k_{in_j}, \tag{12}$$

$$k_{nn_i}^{W(out,out)} = \frac{1}{s_{out_i}} \sum_{j \in V_{out_{(i)}}} w_{ij} k_{out_j}, \tag{13}$$

$$k_{nn_i}^{W(in,out)} = \frac{1}{s_{in_i}} \sum_{j \in V_{in_{(i)}}} w_{ji} k_{out_j}, \tag{14}$$

$$k_{nn_i}^{W(out,in)} = \frac{1}{s_{out_i}} \sum_{j \in V_{out_{(i)}}} w_{ij} k_{in_j}, \tag{15}$$

where all symbols follow those in equations (8)–(11). W indicates that we are dealing with the weighted definition, and the normalization factor is $1/s_i$. The local weight between nodes is now taken into consideration. Equations (12)–(15)

Table 8. Global Network Measures for Directed Virtual Water Trade Networks

		Crop								
	Symbol	Barley	Corn	Rice	Soy	Wheat	Beef	Pork	Poultry	Aggregate
Active export nodes	N_{out}	126	133	127	116	138	116	102	101	151
Active import nodes	N_{in}	166	166	165	166	166	166	166	163	166
Global flow (m^3 yr^{-1})	g	30.5×10^9	62.9×10^9	52.9×10^9	241×10^9	137×10^9	59.2×10^9	19.7×10^9	21.6×10^9	625×10^9
Number of links	L	2852	1974	2124	1999	3376	2154	2005	1708	6033
Average export degree	$\langle k_{out} \rangle$	16.30	11.10	12.14	11.42	18.97	12.52	11.86	10.17	32.79
Average import degree	$\langle k_{in} \rangle$	16.30	11.10	12.14	11.42	18.97	12.52	11.86	10.17	32.79
Maximum export degree	k_{out}^{max}	147	140	131	123	150	108	118	134	159
Maximum import degree	k_{in}^{max}	75	54	37	35	82	43	40	38	97
Average export strength (m^3 yr^{-1})	$\langle s_{out} \rangle$	99.0×10^6	0.35×10^9	0.30×10^9	1.38×10^9	0.77×10^9	0.34×10^9	0.12×10^9	0.13×10^9	3.40×10^9
Average import strength (m^3 yr^{-1})	$\langle s_{out} \rangle$	99.0×10^6	0.35×10^9	0.30×10^9	1.38×10^9	0.77×10^9	0.34×10^9	0.12×10^9	0.13×10^9	3.40×10^9
Maximum export strength (m^3 yr^{-1})	s_{out}^{max}	7.23×10^9	30.8×10^9	17.0×10^9	67.2×10^9	36.2×10^9	12.8×10^9	6.19×10^9	8.36×10^9	165×10^9
Maximum import strength (m^3 yr^{-1})	s_{in}^{max}	4.26×10^9	10.2×10^9	6.14×10^9	24.1×10^9	9.94×10^9	10.5×10^9	3.45×10^9	3.33×10^9	52.1×10^9
Clustering coefficient export	c_{out}	0.40	0.31	0.24	0.25	0.40	0.25	0.29	0.24	0.51
Clustering coefficient import	c_{in}	0.72	0.59	0.55	0.64	0.69	0.59	0.69	0.64	0.74
Clustering coefficient cyclic	c_{cyc}	0.07	0.05	0.03	0.03	0.07	0.04	0.04	0.03	0.09
Clustering coefficient middleman	c_{mid}	0.11	0.10	0.08	0.07	0.11	0.08	0.08	0.07	0.13
Clustering coefficient export random	$c_{ER_{out}}$	0.13	0.08	0.10	0.10	0.14	0.11	0.12	0.10	0.22
Clustering coefficient import random	$c_{ER_{in}}$	0.10	0.07	0.07	0.07	0.11	0.08	0.07	0.06	0.20
Clustering coefficient cyclic random	$c_{ER_{cyc}}$	0.19	0.12	0.14	0.13	0.21	0.15	0.14	0.12	0.36
Clustering coefficient middleman random	$c_{ER_{mid}}$	0.19	0.12	0.14	0.13	0.21	0.15	0.14	0.12	0.36
Clustering coefficient export weighted	c_{out}^{W}	0.54	0.47	0.41	0.42	0.58	0.46	0.49	0.45	0.73
Clustering coefficient import weighted	c_{in}^{W}	0.90	0.83	0.82	0.88	0.91	0.80	0.88	0.88	0.94
Clustering coefficient cyclic weighted	c_{cyc}^{W}	0.11	0.10	0.04	0.06	0.13	0.07	0.07	0.06	0.16
Clustering coefficient middleman weighted	c_{mid}^{W}	0.19	0.21	0.17	0.17	0.21	0.17	0.17	0.17	0.24
Stretched exponential parameter export	α_{out}	0.30	0.30	0.22	0.26	0.26	0.26	0.26	0.26	0.28
Stretched exponential parameter import	α_{in}	0.34	0.38	0.48	0.44	0.44	0.35	0.35	0.32	0.48

thus measure the effective affinity to connect with high-degree or low-degree neighbors according to the magnitude of the actual interactions and the direction of connection.

[53] Both the unweighted and weighted average nearest-neighbor degrees for our directed network are shown in Figure 6. In all cases, the topological definition (i.e., unweighted) displays disassortative behavior (refer to the dashed lines in Figure 6). Thus, nations in the directed virtual water trade network tend to connect with other nations with different topological characteristics from themselves when only the network topology is considered. In all cases, the addition of weights destroys the disassortative structure exhibited in the unweighted case. Note that the solid lines in Figure 6 all remain constant or increase with k. Here $k_{nn}^{W(in,out)}$ and $k_{nn}^{W(out,out)}$ exhibit the largest increase with k, highlighting the importance of major exporters in the network. Interestingly, the accumulation of weights leads major exporting nations to disproportionately connect with one another. Indeed, Denmark, France, Germany, Italy, Netherlands, the United Kingdom, the United States, and China are the countries with the highest $k_{nn}^{W(out,out)}$ and k_{out} (i.e., these nations are represented by the rightmost point on the solid line in Figure 6d). Thus, including information on the network weights and direction illuminates additional information on the global structure of virtual water trade.

[54] When direction is taken into account, there are eight possible combinations of the clustering coefficient that fall into four categories (see *Fagiolo* [2007] for a complete description and representation): c_{in}, c_{out}, c_{cyc}, and c_{mid}. Connectivity between the import neighbors of node i is measured by c^{in}; c^{out} quantifies the clustering between the export neighbors of node i. For both c^{in} and c^{out} we include all closed triangles, regardless of the direction of the connection between the j, h neighbors of node i. However, direction between the j, h neighbors of node i is considered by c^{cyc}, and c^{mid}. The cyclic clustering coefficient (c^{cyc}) measures triangles that follow the specific ordering pattern $i \rightarrow j \rightarrow h \rightarrow i$ or $i \rightarrow h \rightarrow j \rightarrow i$. The middleman clustering coefficient (c^{mid}) measures triangles with the specific ordering pattern $j \rightarrow i \rightarrow h$ and $j \rightarrow h$ or $h \rightarrow i \rightarrow j$

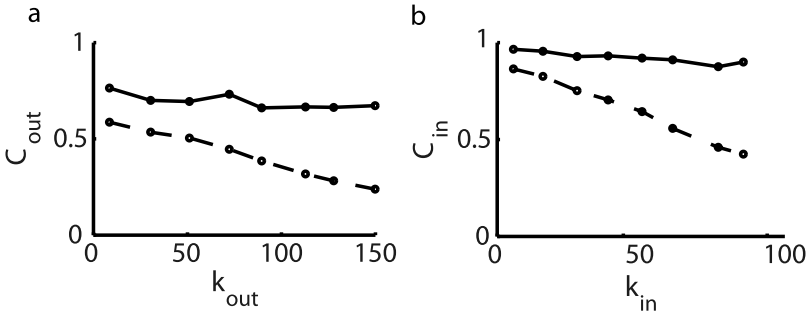

Figure 7. Graphs of the weighted (solid line) and the topological (dashed line) clustering coefficient for the directed network. (a) The out-clustering coefficient (c_{out}) as a function of out-node degree (k_{out}). Refer to (17) and (21) for the unweighted and weighted definition, respectively. (b) The in-clustering coefficient (c_{in}) as a function of in-node degree (k_{in}). Refer to (16) and (20) for the unweighted and weighted definition, respectively. Note that the addition of the network weights destroys the disassortativity observed in the unweighted case in both Figure 7a and Figure 7b.

and $h \rightarrow j$. The explicit equations for the directed clustering coefficients, as given by *Fagiolo* [2007], in the notation used in this paper are

$$c_{\text{in}_i} = \sum_{j,h \in V_{\text{in}_{(i)}}} \frac{(a_{ji} + a_{hi}) a_{jh|hj}}{2 \cdot k_{\text{in}_i}(k_{\text{in}_i} - 1)}, \tag{16}$$

$$c_{\text{out}_i} = \sum_{j,h \in V_{\text{out}_{(i)}}} \frac{(a_{ij} + a_{ih}) a_{jh|hj}}{2 \cdot k_{\text{out}_i}(k_{\text{out}_i} - 1)}, \tag{17}$$

$$c_{\text{cyc}_i} = \sum_{j \in V_{\text{out}_{(i)}}} \sum_{h \in V_{\text{in}_{(i)}}} \frac{(a_{ij} + a_{hi}) a_{jh}}{k_{\text{tot}_i}(k_{\text{tot}_i} - 1)}, \tag{18}$$

$$c_{\text{mid}_i} = \sum_{j \in V_{\text{in}_{(i)}}} \sum_{h \in V_{\text{out}_{(i)}}} \frac{(a_{ih} + a_{ji}) a_{jh}}{k_{\text{tot}_i}(k_{\text{tot}_i} - 1)}, \tag{19}$$

where $a_{jh\backslash hj}$ indicates that a closed triangle is formed if a link exists ($j \rightarrow h$ or $h \rightarrow j$). For this reason, c^{in} and c^{out} are divided by two in the above equations to avoid double counting closed triangles. We define $k_{\text{tot}} = k_{\text{in}} + k_{\text{out}}$ and $s_{\text{tot}} = s_{\text{in}} + s_{\text{out}}$.

[55] When weights are taken into account, the definitions for the directed clustering coefficients as given above become

$$c^{W}_{\text{in}_i} = \sum_{j,h \in V_{\text{in}_{(i)}}} \frac{(w_{ji} + w_{hi}) a_{jh|hj}}{2 s_{\text{in}_i}(k_{\text{in}_i} - 1)}, \tag{20}$$

$$c^{W}_{\text{out}_i} = \sum_{j,h \in V_{\text{out}_{(i)}}} \frac{(w_{ij} + w_{ih}) a_{jh|hj}}{2 s_{\text{out}_i}(k_{\text{out}_i} - 1)}, \tag{21}$$

$$c^{W}_{\text{cyc}_i} = \sum_{j \in V_{\text{out}_{(i)}}} \sum_{h \in V_{\text{in}_{(i)}}} \frac{(w_{ij} + w_{hi}) a_{jh}}{s_{\text{tot}_i}(k_{\text{tot}_i} - 1)}, \tag{22}$$

$$c^{W}_{\text{mid}_i} = \sum_{j \in V_{in_{(i)}}} \sum_{h \in V_{\text{out}_{(i)}}} \frac{(w_{ih} + w_{ji}) a_{jh}}{s_{\text{tot}_i}(k_{\text{tot}_i} - 1)}, \tag{23}$$

where all symbols follow those in equations (16)–(19). W indicates that we are dealing with the weighted definition. The local weight between nodes is now taken into consideration. Equations (20)–(23) thus measure clustering in the network according to the magnitude of the actual interactions between nodes and the direction of connection.

[56] Mean values for each of the four clustering combinations are provided in Table 8. The mean cyclic and middleman clustering coefficients are lower than we would expect in a random network, where $\langle c_{\text{ER}_{\text{mid}}} \rangle$ and $\langle c_{\text{ER}_{\text{cyc}}} \rangle = \langle k_{\text{tot}} \rangle / N_{\text{tot}}$. Even when weights are taken into account, these clustering combinations occur less frequently in the network than would be expected by pure chance. For this reason, we focus our attention on c^{in} and c^{out}; $c^{W}_{\text{out}} > c_{\text{out}} > c_{\text{ER}_{\text{out}}}$ and $c^{W}_{\text{in}} > c_{\text{in}} > c_{\text{ER}_{\text{in}}}$. Thus, the in- and out-clustering patterns occur more frequently in the food trade network than would be expected under pure chance, and the addition of weights increases such clustering.

[57] Figure 7 shows the unweighted, directed clustering coefficient and the weighted, directed clustering coefficient plotted against node degree. From Figure 7, we see that the unweighted clustering coefficient exhibits disassortivity, similar to the undirected case. When weights are included in the definition, the disassortivity breaks down, indicating that highly connected nations form tighter cliques when the volume of trade is considered.

[58] We have shown that the disassortative structure breaks down for the directed network, just as it does for the undirected network, when network weights are properly accounted for. Additionally, incorporating direction highlights the tendency for major exporters to preferentially connect with other major exporters when trade volume is accounted for. This is further evidence that the "weighted rich club" phenomenon is in effect.

[59] Destruction of the disassortative structure with the addition of network weights is also a sign that a network "backbone" exists [*DeMontis et al.*, 2007]. A backbone of a network is a subnetwork comprising only the dominant links [*Glattfelder and Battiston*, 2009]. Following *Glattfelder and Battiston* [2009], we define the backbone of the global virtual water trade network as the core subnetwork where most of the weight resides. Here we choose a threshold value of 80%, so our backbone network comprises only the

largest links that account for 80% of the flow volume. This results in the removal of the weakest links and any resulting isolated nodes. Surprisingly, 80% of the global flow is captured with only 255 links, or 4.2% of the links in the complete network. This backbone forms a single connected component, which indicates that all of the nodes in the backbone network are connected. The backbone consists of 79 nodes that export and 37 that import, compared to 151 export nodes and 166 import nodes in the complete network. It is interesting that there are more export nodes in the backbone network, while there are more import nodes in the complete network.

[60] This provides a clear picture in which dominant and highly connected nations participate in large-volume trade with one another, while a large number of small countries are on the trade periphery and are connected to these hubs and each other through trade of relatively small volumes.

4. Conclusions

[61] In this paper we applied a novel conceptual and methodological framework to the study of global virtual water trade. The virtual water trade that we analyzed was that associated with the international food trade (i.e., 58 commodities from five major crops and three livestock types). These food products account for 60% of global calorie consumption. The main motivation of this study was to obtain empirical knowledge of the global network structure.

[62] Quantifying the global structure is important for the understanding and management of any system, which here is the linked water and food trade. Our analysis quantifies the topology of the international food trade, an often discussed topic in the policy community, finding that export trade connections follow an exponential distribution. We also characterized the weighted features of the network architecture as given by virtual water flows, which was found to follow a stretched exponential distribution. These probability distributions provide water resource professionals with an accurate description of the system.

[63] We highlight how individual nations fit into the global structure, which enables national policy makers to determine the relationship of their country to the international community. The United States is the dominant exporter of virtual water, while Japan is the major importer. The trade of virtual water from the United States to Japan alone accounts for 5% of global virtual water flow. The United States, France, and Netherlands occupy important roles in the global structure. The trade volume exhibits a power law relationship with the number of trade partners of each nation, indicating that the more trading partners a country has, the much more virtual water it trades, particularly in terms of import trade relationships. This finding has important implications for the trade policy of water-scarce nations looking to increase their access to water resources.

[64] This analysis provided evidence for the existence of the weighted rich club phenomenon, where a tightly clustered group of countries trade the majority of the resources among themselves. This network structure exists with or without direction. However, major exporters preferentially trade large volumes of virtual water with one another. We uncovered a global trading hierarchy, in which a few dominant nations connect otherwise disconnected portions of the network and form tight clusters with each other. The majority of the nations reside on the periphery of the trade network and participate in relatively small volume trade.

[65] Applying the analytical tools of complex network theory to virtual water trade provides important insights into its global architecture. This empirical analysis, while interesting in its own right, is the necessary first step for developing and validating modeling approaches. Additionally, we believe that this analysis opens the way for many possible extensions with practical applications, such as community detection; mapping change over time; and understanding systemic risk, particularly under the potential impacts of climate change, as well as opportunities for network optimization.

[66] **Acknowledgments.** We acknowledge the Food and Agricultural Organization for making available the global agricultural trade data. M.K. acknowledges the support of the National Science Foundation (NSF) Graduate Research Fellowship Program (GRFP) and the James S. McDonnell Foundation; C.D. and I.R.-I. acknowledge the support of the James S. McDonnell Foundation; and S.S. and A.R. acknowledge funding from ERC advanced grant RINEC 22761 and SFN grant 200021/124930/1.

References

Allan, T. (1993), Fortunately there are substitutes for water: Otherwise our hydropolitical futures would be impossible, paper presented at Conference on Priorities for Water Resources Allocation and Management, Overseas Dev. Admin., London.

Barabási, A.-L. (2002), *Linked: The New Science of Networks*, Perseus, Cambridge, Mass.

Barabási, A.-L., and R. Albert (1997), Emergence of scaling in random networks, *Science*, *286*, 509–512.

Barigozzi, M., G. Fagiolo, and D. Garlaschelli (2010), Multinetwork of international trade: A commodity-specific analysis, *Phys. Rev. E*, *81*, 046104.

Barrat, A., M. Barthelemy, R. Pastor-Satorras, and A. Vespignani (2004), The architecture of complex weighted networks, *Proc. Natl. Acad. Sci. U. S. A.*, *101*(11), 3747–3752.

Barthelemy, M. (2004), Betweenness centrality in large complex networks, *Eur. Phys. J. B*, *38*(2), 163–168.

Boguna, M., and R. Pastor-Satorras (2003), Class of correlated random networks with hidden variables, *Phys. Rev. E*, *68*, 036112.

Bollobás, B. (1985), *Random Graphs*, 1st ed., Academic, New York.

Chapagain, A. K., and A. Y. Hoekstra (2008), The global component of freshwater demand and supply: An assessment of virtual water flows between nations as a results of trade in agricultural and industrial products, *Water Int.*, *33*(1), 19–32.

Chapagain, A. K., A. Hoekstra, and H. Savenije (2006), Water saving through international trade of agricultural products, *Hydrol. Earth Syst. Sci.*, *10*, 455–468.

Costa, L., F. Rodrigues, G. Travieso, and P. V. Boas (2007), Characterization of complex networks: A survey of measurements, *Adv. Phys.*, *56*(1), 167–242.

DeMontis, A., M. Barthelemy, A. Chessa, and A. Vespignani (2007), The structure of interurban traffic: A weighted network analysis, *Acta Math. Sci. Hung.*, *34*, 905–924.

D'Odorico, P., F. Laio, and L. Ridolfi (2010), Does globalization of water reduce societal resilience to drought?, *Geophys. Res. Lett.*, *37*, L13403, doi:10.1029/2010GL043167.

Erdös, P., and A. Rényi (1961), On random graphs, *Acta Math. Sci. Hung.*, *12*, 261–267.

Fagiolo, G. (2007), Clustering in complex directed networks, *Phys. Rev. E*, *76*, 026107.

Fagiolo, G., J. Reyes, and S. Schiavo (2008), On the topological properties of the world trade web: A weighted network analysis, *Physica A*, *387*, 3868–3873.

Falkenmark, M., and J. Rockstrom (2004), *Balancing Water for Humans and Nature*, Earthscan, London.

Foster, J., D. Foster, P. Grassberger, and M. Paczuski (2010), Edge direction and the structure of networks, *Proc. Natl. Acad. Sci. U. S. A.*, *107*(24), 10,815–10,820.

Garlaschelli, D., and M. I. Loffredo (2005), Structure and evolution of the world trade network, *Physica A*, *355*, 491–499.

Gerbens-Leenes, W., A. Y. Hoekstra, and T. H. van der Meer (2009), The water footprint of bioenergy, *Proc. Natl. Acad. Sci. U. S. A.*, *106*(25), 10,219–10,223.

Glattfelder, J., and S. Battiston (2009), Backbone of complex networks of corporations: The flow of control, *Phys. Rev. E*, *80*(3), 036104.

Gleick, P. (2008), *The World's Water 2008–2009: The Biennial Report on Freshwater Resources*, 1st ed., Island, Washington, D. C.

Hanasaki, N., S. Kanae, T. Oki, K. Masuda, N. Shirakawa, Y. Shen, and K. Tanaka (2008a), An integrated model for the assessment of global water resources—Part 1: Model description and input meteorological forcing, *Hydrol. Earth Syst. Sci.*, *12*, 1007–1025.

Hanasaki, N., S. Kanae, T. Oki, K. Masuda, K. Motoya, N. Shirakawa, Y. Shen, and K. Tanaka (2008b), An integrated model for the assessment of global water resources—Part 2: Applications and assessments, *Hydrol. Earth Syst. Sci.*, *12*(3–4), 1027–1037.

Hanasaki, N., T. Inuzuka, S. Kanae, and T. Oki (2010), An estimation of global virtual water flow and sources of water withdrawal for major crops and livestock products using a global hydrological model, *J. Hydrol.*, *384*(3–4), 232–244.

Hoekstra, A., and A. Chapagain (2008), *Globalization of Water: Sharing the Planet's Freshwater Resources*, Blackwell, Malden, Mass.

Hoekstra, A., and P. Hung (2005), Globalisation of water resources: International virtual water flows in relation to crop trade, *Global Environ. Change*, *15*, 45–56.

Jackson, M. (2008), *Social and Economic Networks*, Princeton Univ. Press, Princeton, N. J.

Kalapala, V., V. Sanwalani, A. Clauset, and C. Moore (2006), Scale invariance in road networks, *Phys. Rev. E*, *73*, 026130.

Krzywinski, M. (2009), Circos: An information aesthetic for comparative genomics, *Genome Res.*, *19*, 1639–1645.

Kyriakopoulos, F., S. Thurner, C. Puhr, and S. W. Schmitz (2009), Network and eigenvalue analysis of financial transaction networks, *Eur. Phys. J. B*, *71*, 523–531.

Liu, J., J. R. Williams, A. J. Zehnder, and H. Yang (2007), GEPIC—Modelling wheat yield and crop water productivity with high resolution on a global scale, *Agric. Syst.*, *94*, 478–493.

Ma, J., A. Hoekstra, H. Wang, A. Chapagain, and D. Wang (2006), Virtual versus real water transfers within China, *Philos. Trans. R. Soc. B*, *361*, 835–842.

Masucci, A., D. Smith, A. Crooks, and M. Batty (2009), Random planar graphs and the London street network, *Work. Pap. Ser. 146*, Univ. Coll., London, London.

Miguens, J., and J. Mendes (2008), Weighted and directed network on traveling patterns, *Biowire*, *5151*, 145–154.

Newman, M. (2001), Scientific collaboration networks: 1. Network construction and fundamental results, *Phys. Rev. E*, *64*, 016131.

Newman, M. (2003), The structure and function of complex networks, *Siam Rev.*, *45*, 167–256.

Newman, M., A.-L. Barabási, and D. J. Watts (2006), *The Structure and Dynamics of Networks*, 1st ed., Princeton Univ. Press, Princeton, N. J.

Oki, T., and S. Kanae (2004), Virtual water trade and world water resources, *Water Sci. Technol.*, *49*(7), 203–209.

Opsahl, T., V. Colizza, P. Panzarasa, and J. Ramasco (2008), Prominence and control: The weighted rich-club effect, *Phys. Rev. L*, *101*, 168702.

Pastor-Satorras, R., A. Vazquez, and A. Vespignani (2001), Dynamical and correlation properties of the internet, *Phys. Rev. Lett.*, *87*, 258701.

Rost, S., D. Gerten, A. Bondeau, W. Lucht, J. Rohwer, and S. Schaphoff (2008), Agicultural green and blue water consumption and its influence on the global water system, *Water Resour. Res.*, *44*, W09405, doi:10.1029/2007WR006331.

Shiklomanov, I. (1997), Assessment of water resources and water availability in the world. Background report for the comprehensive assessment of the freshwater resources of the world, Stockholm Environ. Inst., Stockholm.

Strzepek, K., and B. Boehlert (2010), Competition for water for the food system, *Philos. Trans. R. Soc. B*, *365*, 2927–2940.

Suweis, S., M. Konar, C. Dalin, A. Rinaldo, and I. Rodriguez-Iturbe (2011), Structure and controls of the global virtual water trade network, *Geophys. Res. Lett.*, doi:10.1029/2011GL046837, in press.

Verma, S., D. Kampman, P. van der Zaag, and A. Hoekstra (2009), Going against the flow: A critical analysis of virtual water trade in the context of India's national river linking program, *Phys. Chem. Earth*, *34*, 261–269.

Vorosmarty, C., P. Green, J. Salisbury, and R. Lammers (2000), Global water resources: vulnerability from climate change and population growth, *Science*, *289*, 284–288.

Wasserman, S., and K. Faust (1994), *Social Network Snalysis: Methods and Applications*, 1st ed., Cambridge Univ. Press, Cambridge, U. K.

Watts, D. J., and S. H. Strogatz (1998), Collective dynamics of small-world networks, *Nature*, *393*(6684), 440–442.

Wilks, D. S. (2006), *Statistical Methods in the Atmospheric Sciences*, 2nd ed., Academic, Amsterdam.

Yang, H., L. Wang, K. Abbaspour, and A. Zehnder (2006), Virtual water trade: An assessment of water use efficiency in the international food trade, *Hydrol. Earth Syst. Sci.*, *10*, 443–454.

C. Dalin, M. Konar, and I. Rodriguez-Iturbe, Department of Civil and Environmental Engineering, Princeton University, Engineering Quad, Princeton, NJ 08544, USA. (cdalin@princeton.edu; mkonar@princeton.edu; irodrigu@princeton.edu)

N. Hanasaki, National Institute for Environmental Studies, 16-2 Onogawa, Tsukuba, Ibaraki 305-8506, Japan. (hanasaki@nies.go.jp)

A. Rinaldo and S. Suweis, Laboratory of Ecohydrology, ECHO/IEE/ENAC, École Polytechnique Fédérale de Lausanne, CH-1015, Lausanne, Switzerland. (andrea.rinaldo@epfl.ch; samir.suweis@epfl.ch)